

PROCEEDINGS OF SPIE

[SPIDigitalLibrary.org/conference-proceedings-of-spie](https://spiedigitallibrary.org/conference-proceedings-of-spie)

Single detector imaging lidar by digital micromirror device for large field-of-view and mid-range mapping applications

Brandon Hellman, Adley Gin, Braden Smith, Young-Sik Kim, Guanghao Chen, et al.

Brandon Hellman, Adley Gin, Braden Smith, Young-Sik Kim, Guanghao Chen, Paul Winkler, Phillip McCann, Yuzuru Takashima, "Single detector imaging lidar by digital micromirror device for large field-of-view and mid-range mapping applications," Proc. SPIE 10757, Optical Data Storage 2018: Industrial Optical Devices and Systems, 107570H (14 September 2018); doi: 10.1117/12.2323878

SPIE.

Event: SPIE Optical Engineering + Applications, 2018, San Diego, California, United States

Single detector imaging lidar by Digital Micromirror Device for large field-of-view and mid-range mapping applications

Brandon Hellman*^a, Adley Gin^a, Braden Smith^{a,b}, Young-Sik Kim^a,
Guanghao Chen^a, Paul Winkler^a, Phillip McCann^a, Yuzuru Takashima^a

^aUniversity of Arizona, 1630 E University Blvd, Tucson, AZ, USA 85721

^bSandia National Laboratories, 1515 Eubank Blvd SE, Albuquerque, NM, USA 87123

ABSTRACT

An imaging lidar system is presented which combines the high speed of a Digital Micromirror Device (DMD) and the higher range of a 1D collimated scanning output. The system employing 1D line object illumination along with DMD placed at focal plane enables flexible optimization of system metrics, such as field of view, angular resolution, maximum range distance and frame rate.

Keywords: Lidar, Imaging lidar, MEMS, DMD, Beam steering

1. INTRODUCTION

Light Detection and Ranging (lidar) systems enable the capture of distance and direction information across a field of view. This 3D mapping has been used to enable autonomous and driver assisted vehicles, fish population mapping, and measurement of gas concentration in the atmosphere^{1,2}. Lidar systems are comprised of a ranging mechanism, necessary to capture the distance information, and a scanning or mapping mechanism, necessary to determine the direction of each distance measurement. A ranging time-of-flight (TOF) measurement is commonly employed where a short pulse is emitted from a transmitter, reflected by a target, and captured by a receiver. The time-of-flight of the pulse is measured to determine the distance of the target³. Other types of ranging schemes exist, including frequency modulation, coded waveforms, heterodyne detection, and gated capture, but the same radiometric principles apply. Regardless of the ranging scheme, the type of scanning and mapping mechanisms drastically affects system performance such as maximum ranging distance, field of view, angular resolution and scan speed. Those scanning modalities, although widely varying, are categorized into three major schemes from the radiometry perspective. In this paper, we review radiometry of lidar systems, and introduce a high speed and midrange lidar system by employing a Digital Micromirror Device (DMD) as a part of receiver. We present an imaging lidar system which combines the wide-angle beam steering radiometric benefit of a mechanical rotating galvo mirror with the high-speed light filtering capabilities of the DMD.

2. LIDAR RADIOMETRY

Radiometric principles can be applied to different lidar scanning or mapping mechanisms to determine their photon efficiencies^{3,4}. For instance, a ‘flood’ illumination scheme emits light across the entire field-of-view of the lidar system, diverging the light in two dimension from transmitter (Fig. 1a). We consider a single laser pulse for time of flight (TOF) –based lidar. The total energy per pulse, per area E_0 scales with $1/R^2$, consequently, the energy per pulse, per area at an object E_1 decreases by factor of $1/R^2$ (Fig. 1a), where R is the distance from transmitter to object. The irradiance back at the entrance aperture of the receiver, after an assumed Lambertian reflection, will be proportional to $1/R^2$ times the irradiance at the target. This means the overall photo efficiency is proportional to $1/R^4$ for the flood illumination scheme.

For a beam steering illumination scheme with a collimated beam, divergence of the beam is negligible. The irradiance at the target will be proportional to the irradiance at the exit aperture of the transmitter, independent of R ignoring scatter and absorption by air. The Lambertian reflected signal will maintain its $1/R^2$ efficiency on the return trip to the receiver, for an overall photon efficiency and signal drop-off proportional to $1/R^2$.

*hellman@email.arizona.edu

Optical Data Storage 2018: Industrial Optical Devices and Systems, edited by Ryuichi Katayama,
Yuzuru Takashima, Proc. of SPIE Vol. 10757, 107570H · © 2018 SPIE
CCC code: 0277-786X/18/\$18 · doi: 10.1117/12.2323878

Proc. of SPIE Vol. 10757 107570H-1

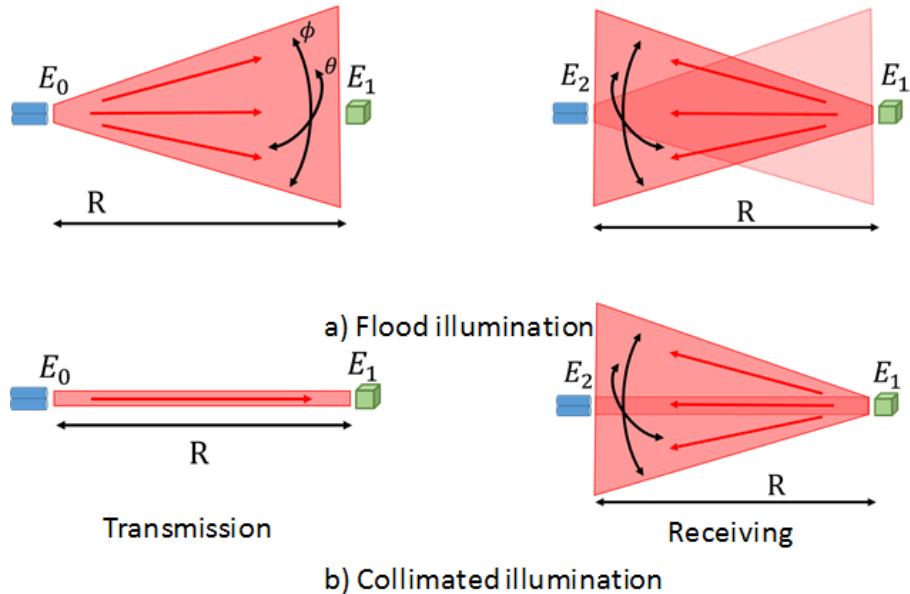


Figure 1. Transmitted signal efficiency for a) a flood beam and a b) collimated beam.

While this higher efficiency is necessary for long range distance measurement, lidar systems with collimated illumination are necessary for high-speed vehicles. In these systems, a point-by-point scanning mechanism, typically on a rotating stage where both the transmitter and receiver are placed, is necessary, though the system can take significant time to scan across the thousands of points. This is the tradeoff between the high speed of a flood system and the high max range of a collimated illumination system. In contrast, the flood illumination system has no moving parts at the expense of maximum measurable distance due to the $1/R^4$ efficiency drop.

3. OPTICAL ARCHITECTURE

The lidar system schematically depicted in Fig. 2 is a midpoint, “ $1/R^3$ ”, solution between the collimated and two-dimensional diverging illumination schemes. The system uses a one-dimensional collimated beam for an overall $1/R^3$ system photon efficiency. This avoids the slow speed of a two-axes beam steering system while surpassing the $1/R^4$ photon efficiency of a flood illumination scheme. While the one-axis galvo mirror is slow compared to single-shot systems, the second axis scan is achieved by a Digital Micromirror Device, enabling kHz sample rates.

The system is comprised of a transmitter and a receiver. The transmitter includes a short pulse source laser, a collimating lens, a diffuser, and a cylindrical lens to output a 0.5° (H) \times 10° (V) beam through a one-dimensional scanning galvo mirror rotating across a 35° range for a total output coverage area of 70° (H) \times 10° (V). The receiver includes an imaging lens to image the field-of-view across a DMD which filters out all light except a horizontal line across the field-of-view corresponding to a 70° (H) \times 0.5° (V) field filter. The horizontally-steerable vertical illumination line coupled with the vertically-programmable filter enables a two-axis raster scanning of the field. For each field point, the reflected signal from the field is collected by a relay lens and funneled into an Avalanche Photodiode (APD) for signal detection.

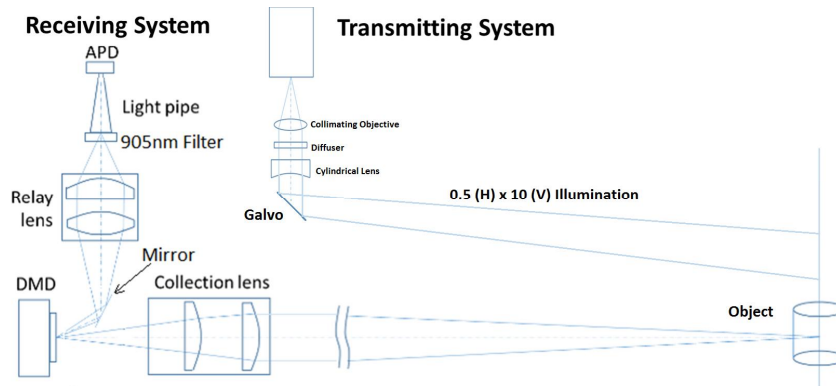


Figure 2. Optical architecture of the imaging lidar by employing a DMD in the receiver

4. PERFORMANCE

In Table 1, the experimentally confirmed performances are summarized. The system has various tradeoffs between specifications. We tested setup parameters, such as DMD and galvo programming, and found how each spec could be individually maximized to a “Best Demonstrated”, or the overall system could be balanced for an “Optimized System” as shown Table 1.

Table 1. System performance, including the best demonstrated individual spec and the overall optimized system.

Specification	Best Demonstrated	Optimized System	Tradeoff
1. Maximum distance	7.5 m	5 m	FOV vs. distance
2. Distance resolution		6.8 cm	(Chipset limited)
3. Field-of-View (HxV)	70 ⁰ x10 ⁰	50 ⁰ x10 ⁰	FOV vs. distance
4. Angular resolution (HxV)	0.5 ⁰ x0.5 ⁰	0.5 ⁰ x1 ⁰	Resolution vs. distance Resolution vs. scan rate
5. Frame rate	8.4 FPS	5.6 FPS	Resolution vs. scan rate
6. System size	NA	12”x12”x4”	(Excluding peripherals)

3.1 Maximum distance

The max distance has a trade-off with field of view (FOV). This can be understood that aperture size of the collection lens. The system uses a c-mount zoom lens. While increasing the FOV, the entrance pupil diameter decreases which decreases number of photons captured by the receiver.

3.2 Distance resolution

Figure 3a depicts the distance resolution test. Targets were placed at a set distance in the FOV of the lidar system, and a center target was incrementally shifted forward and back from the original location to capture different distance measurements. The electronics do not capture direct distance information, but rather a raw number corresponding to a time duration. While this time is ideally accurate after the on-chip calibration, we found the picosecond resolution timer to require additional calibration. We calibrated the time measurements for different target distances to the measured distances, and found a root-sum-square residual error corresponding to the overall distance resolution.

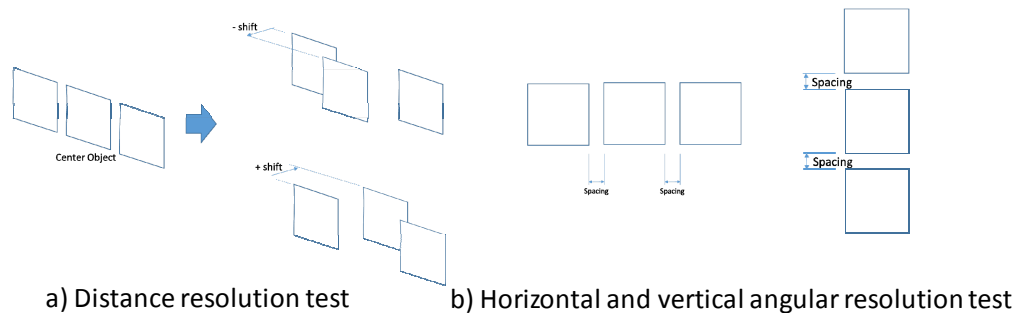


Figure 3. a) Distance resolution test: targets incrementally separated along the line-of-sight in the field-of-view, b) Angular resolution testing: targets incrementally separated horizontally and vertically

3.3 Field of View

As discussed in 3.1, FOV has a trade-off to the maximum distance. While $70^{\circ} \times 10^{\circ}$ (HxV) is feasible, we found that $50^{\circ} \times 10^{\circ}$ can accommodate the maximum distance of 5m of our target.

3.4 Angular resolution, Maximum distance and Frame rate trade-off

In order to test the horizontal angular resolution of the system, a test scenario was implemented. Figure 3b shows a schematic view of test targets from the lidar system of the targets.

25x25mm and 50x50mm white paper cards were used as as high reflectivity targets, and cardboard cards of the same dimensions were used for low reflectivity targets. Three targets were arranged with straight vertical and horizontal edges adjacent to one another in the field of view to test horizontal and vertical resolution (Fig. 3a). The system captured data from the field of view, and then the targets were incrementally separated in the horizontal, vertical, and line-of-sight dimensions (Fig. 3b), with lidar system captures between increments. The minimum spacing required to resolve that a gap exists in the target wall can be used with the distance of the targets to determine the horizontal angular resolution of the system.

Since the DMD is placed closer to the back focal point of the collection lens, the DMD is spatial filter which is conjugate to the object. The focal length of the collection lens is on the order of tens of millimeters, which is much smaller than the object distance. Under this condition, all the objects are in-focus. This condition assures that the DMD can select a vertical region of the object in a programmable manner such that resolution and fill-factor of the pixels are independently controllable.

Figure 4 schematically depicts the functionality of the DMD as an adoptive vertical spatial filter. For example, at a time of t , a laser line illuminates column i and row j of DMD is turned on. The object imaged onto the DMD is sampled at position (i,j) corresponding to a 0.5×0.5 degree field point. Once the position (i, j) is sampled, the next row $j+1$ of the DMD pixel is turned on, the position $(i, j+1)$ is sampled, and so on (Fig. 4a). This sampling can be considered as a normal sampling; the vertical pixel size and sampling pitch are equal, and the fill factor of the DMD is 100%. The optical architecture enables samples with even higher fill factor than 100% as depicted in Fig. 4b. The high fill factor sampling has a benefit in increasing the maximum distance while not penalizing horizontal resolution, at an expense of reduced vertical resolution. The sampling pitch can be also used to optimize frame rate.

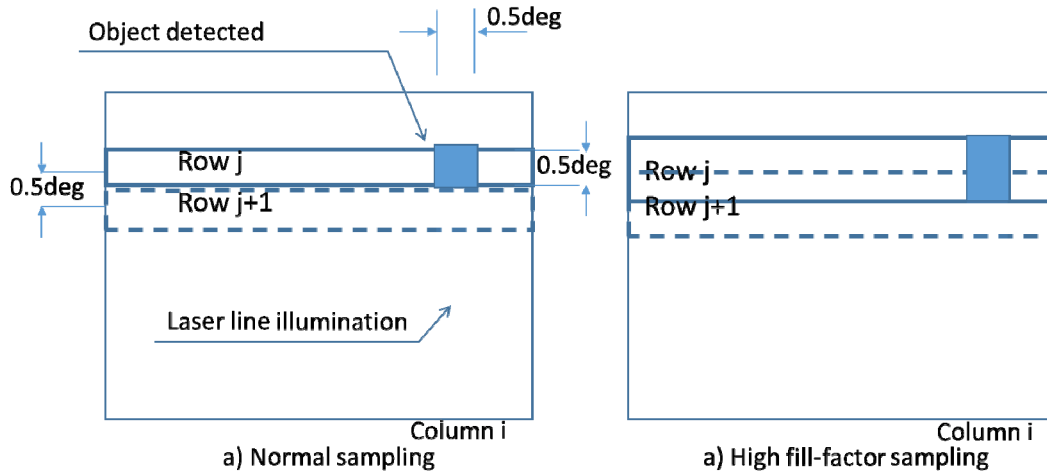


Figure 4. Functionality of the DMD as an adoptive vertical spatial filter

In Fig. 4, we explained our method of adaptive vertical sampling of the image on the DMD plane. A that similar adoptive sampling in the horizontal direction can be done with Galvo. While the transmitter has a fixed output beam, 0.5° (H) \times 10° (V), the galvo itself is programmable. This means over-sampling, by incrementing output from the galvo by less than 0.5° in the horizontal dimension, or under-sampling, by incrementing the galvo by greater than 0.5° in the horizontal dimension, can have an effect on the number of sample points and the angular resolution of the system. An example of range finding result of multiple targets with in 70×10 (HxV) field of view is shown in Fig. 5.

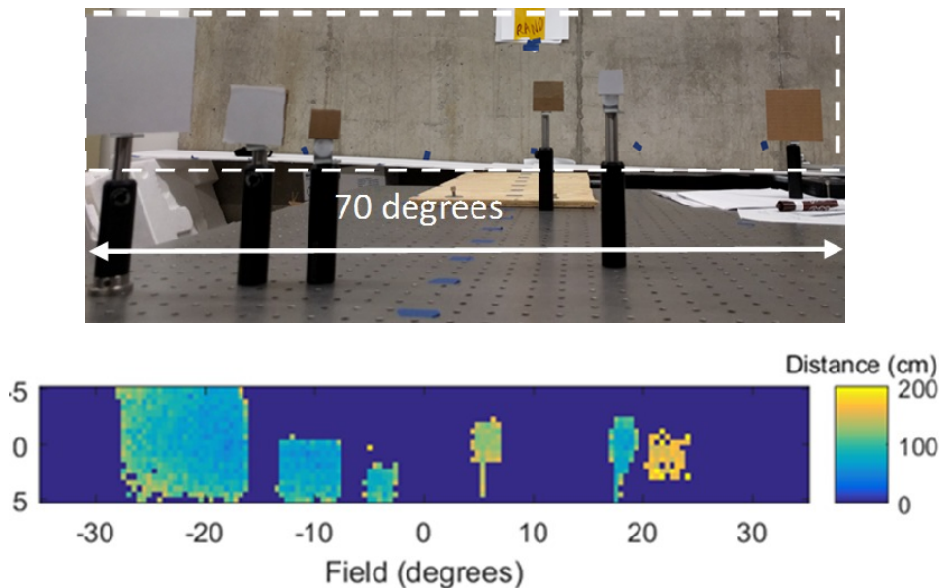


Figure 5. Targets across the field-of-view of the lidar system (top), and lidar capture (bottom).

5. CONCLUSIONS

We have demonstrated a mid-point solution using a 1D collimated, beam steered illumination scheme coupled with an imaging receiver using a DMD-based spatial filter for a second axis of high-speed scanning. We developed testing metrics to determine system performance, and varied system parameters to produce an overall optimized system. The system achieved a field of view of 50x10 degrees, an angular resolution of 0.5x1 degrees, and a maximum ranging distance of 5m while sustaining a frame rate of 5.6 frames per second.

REFERENCES

- [1] K. Bimbray, "Autonomous cars: Past, present and future a review of the developments in the last century, the present scenario and the expected future of autonomous vehicle technology," 2015 12th International Conference on Informatics in Control, Automation and Robotics (ICINCO), Colmar, 2015, pp. 191-198.
- [2] J. Shaw, "Lidar Instruments and Applications," in Conference on Lasers and Electro-Optics, OSA Technical Digest (online) (Optical Society of America, 2017), paper SW4L.1.
- [3] Paul McManamon, *Field Guide to Lidar*, SPIE Press, 2015.
- [4] J. Palmer; Barbara Grant, *The Art of Radiometry*, SPIE Press, 2009.